

# Engineering Notes

ENGINEERING NOTES are short manuscripts describing new developments or important results of a preliminary nature. These Notes cannot exceed 6 manuscript pages and 3 figures; a page of text may be substituted for a figure and vice versa. After informal review by the editors, they may be published within a few months of the date of receipt. Style requirements are the same as for regular contributions (see inside back cover).

C80-092

## Lift and Drag Measurements of Two Rotating Cylinders

Georges Bridel\*

Institut für Aerodynamik Eidg. Technische Hochschule  
Zurich, Switzerland

### Introduction

LIFT and drag measurements with two rotating cylinders have been performed in order to test the balance described in Ref. 1 under difficult conditions where relatively small forces had to be measured and mechanical vibrations occurred. Rotating cylinders at an angle of attack create high lift and show a new behavior of the rear stagnation point which is different from the Kutta-Joukowski condition. At the zero lift condition  $\alpha = 90^\circ$  the complete elimination of the pressure drag is realized.

### Potential Flow Analysis

The potential flowfield around two cylinders (Fig. 1) can be described by conformal mapping of the dipole row from the  $\xi$ -plane into the  $z$ -plane with the transformation  $z = -(a/2\xi)$ . The complex potential is

$$\chi(z) = -i w_\infty a \pi \cotan(\pi a/z)$$

If a lift force is generated, the magnitude  $\Gamma$  of the corresponding vortex depends only upon the angle  $\alpha$  of the flow and the angular location  $\varphi_r$  of the rear stagnation point. The potential flow can easily be calculated by superimposing the complex potentials for the selected rear stagnation point location. If the stagnation point is assumed to be located in the slot between the two cylinders, the lift coefficient based on  $b = 4 \cdot a$  in Fig. 1 is

$$C_l = \pi^2 \cos \alpha$$

The maximum theoretical lift coefficient  $c_{lmax} = 9.87$  occurs at  $\alpha = 0^\circ$  and is also the maximum for all other conditions where both stagnation points fall together on one point anywhere on the cylinder surface. Figure 2 shows the lift coefficient as a function of the stagnation point location  $\varphi_r$ . The flowfield and corresponding pressure distribution for  $\varphi_r = 180^\circ$  and  $\alpha = 45^\circ$  are shown in Fig. 3.

### Experimental Setup

The experiments were performed in the subsonic wind tunnel of the ETH which has a  $3 \times 2.1$  m test section.<sup>2</sup> In order to minimize end effects due to separation of the wind tunnel wall boundary layer, a small diameter (0.105 m) had been selected giving a large span (2.1 m) to diameter ratio.

Received Feb. 13, 1979; revision received Nov. 1, 1979. Copyright © American Institute of Aeronautics and Astronautics, Inc., 1979. All rights reserved.

Index categories: Aerodynamics; Jets, Wakes, and Viscid-Inviscid Flow Interactions; Subsonic Flow.

\*Research Engineer. Member AIAA.

The cylinders were made of light alloys with a wall thickness of 1.5 mm in order to avoid large rotating masses. They were driven by a speed-regulated dc motor mounted on the upper end of the vertically installed cylinders.

On the lower end, the cylinders were attached to the wind tunnel balance. Membrane supports on each end helped to separate the aerodynamic forces.<sup>1</sup>

The wind tunnel wall boundary layer tends to separate in the vicinity of the rotating cylinders, thereby creating additional drag. This can be eliminated by suction through

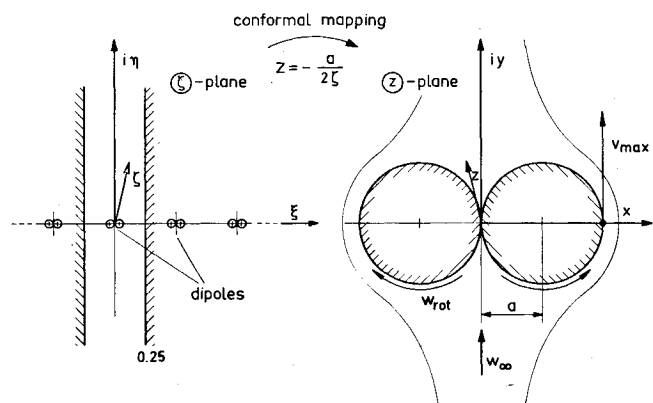


Fig. 1 Basic conformal mapping procedure to obtain a potential flowfield around two cylinders. Under real flow conditions, the flowfield can be achieved by rotating the cylinders.

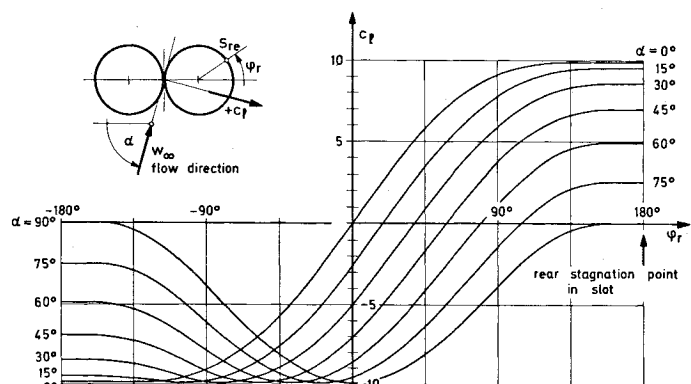


Fig. 2 Lift coefficient  $c_l$  of two cylinders in function of  $\alpha$  and the rear stagnation point location  $\varphi_r$ .

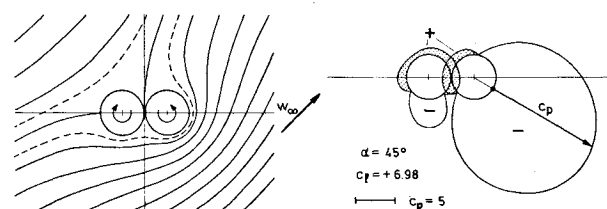


Fig. 3 Potential flowfield and pressure distribution around two cylinders,  $\alpha = 45^\circ$ ;  $\varphi_r = 180^\circ$ .

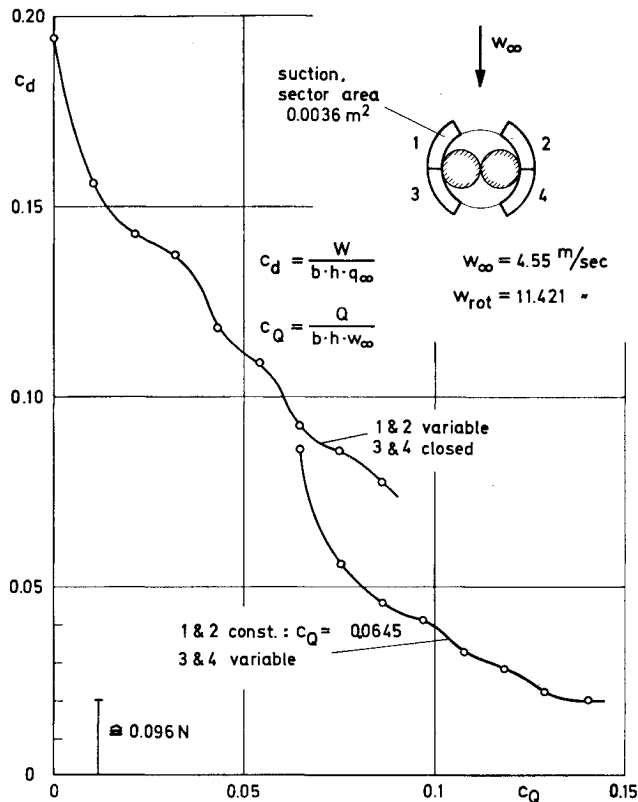


Fig. 4 The remaining drag due to end-wall separation can be eliminated with suction through the wind tunnel wall ( $c_Q$  is indicated for both walls).

perforated sheets attached to the wind tunnel wall. During the investigation it was found that it was most effective to apply the suction very close to the cylinders through relatively small sectors. The drag could in this way be reduced by 90% (Fig. 4).

### Discussion of Results

The drag measurements were made at  $\alpha = 90^\circ$  deg, where the flowfield takes the shape shown in Fig. 1. No flow separation should occur if the potential flow velocity  $v_{\max} = 2.472 w_\infty$  is equal to the rotational speed  $w_{\text{rot}}$ . As the momentum in the

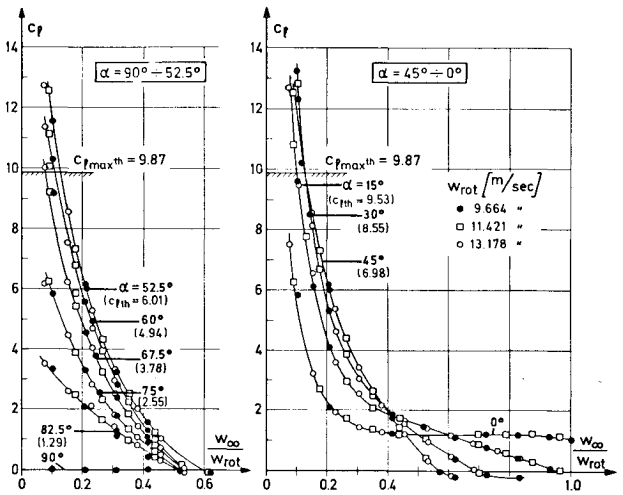
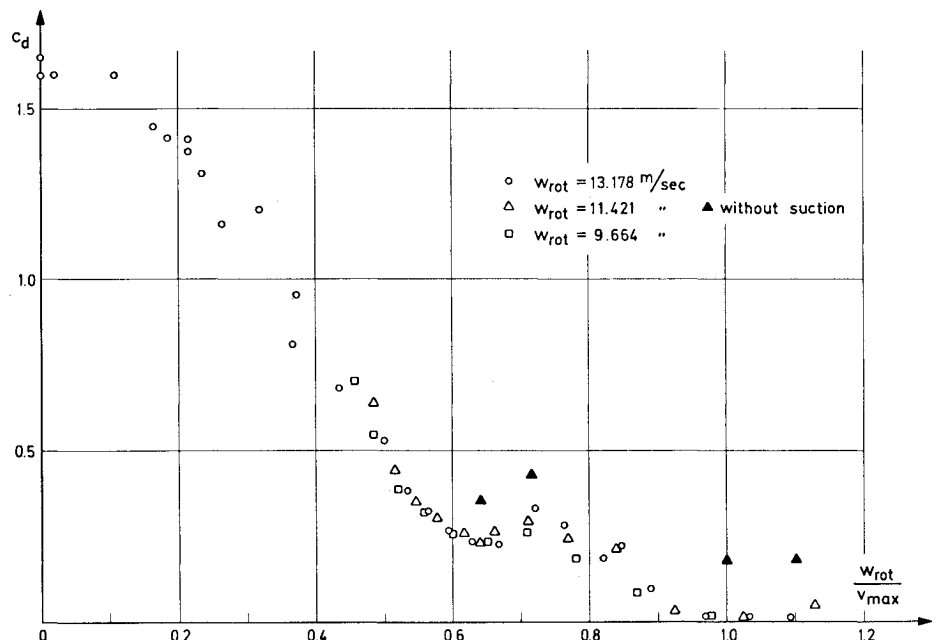


Fig. 6 Lift measurements of the rotating cylinders as a function of  $w_\infty/w_{\text{rot}}$ . Three different rotational speeds have been investigated. Theoretical values  $c_{lth}$  are indicated for  $\phi_r = 180^\circ$  deg.

boundary layer close to  $v_{\max}$  is higher than in the adjacent free flow, a considerably lower value than  $w_{\text{rot}}/v_{\max} = 1$  would be expected before separation of the turbulent boundary layer occurs. However, Fig. 5 shows the drag-rise to start as soon as  $w_{\text{rot}}/v_{\max} < 1$ . The suction arrangement corresponded to the optimum solution where suction is applied in the sectors 1 to 4 (Fig. 4). The rate  $c_Q = 0.14$  for  $w_\infty = 11.421$  remained constant but was adapted for the other rotational speeds. The drag-plateau for  $0.6 < w_{\text{rot}}/v_{\max} < 0.9$  shown in Fig. 5 is not associated with the applied wall suction but is due to a weak vortex-street disappearing below  $w_{\text{rot}}/v_{\max} = 0.6$ . Within the limits of the investigation, drag does not depend on Re but only on the ratio  $w_{\text{rot}}/v_{\max}$  (Fig. 5). If the ratio is increased to values considerably above 1, the wake is replaced by a jet. The resulting thrust could not be clearly measured due to its small magnitude compared to the vibration forces of the rotating cylinders.

The lift measurements were carried out between  $0 \text{ deg} \leq \alpha \leq 90 \text{ deg}$  with three different rotational speeds,  $w_{\text{rot}} = 9.664, 11.421$  and  $13.178 \text{ m/s}$ . The forces and the flowfield depend only on the ratio  $w_\infty/w_{\text{rot}}$ . The point  $c_{lth}$  indicates the theoretical lift coefficient obtained with the rear

Fig. 5 Drag coefficient of two contrarotating cylinders as a function of the rotational speed to the maximum velocity  $w_{\text{rot}}/v_{\max}$  where  $v_{\max} = 2.472 w_\infty$ .



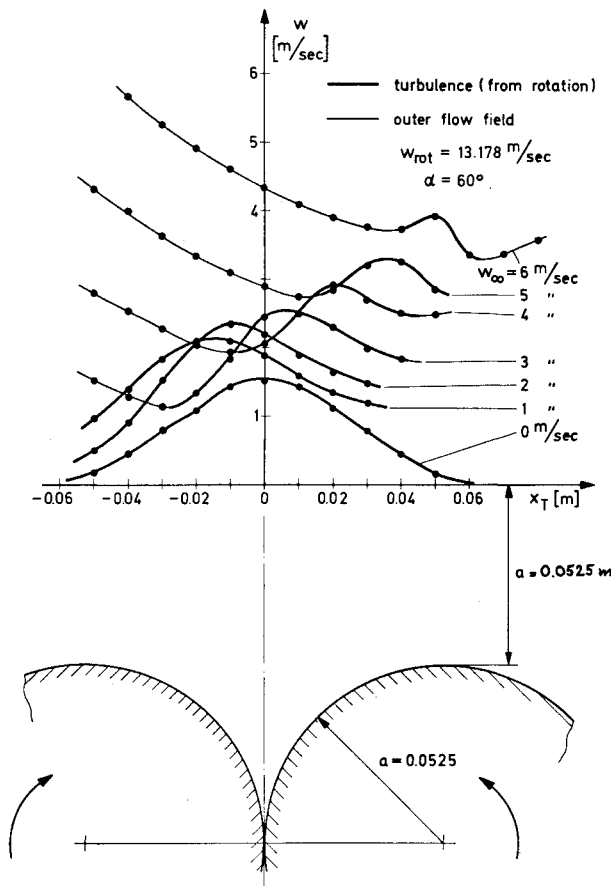


Fig. 7 Velocity distribution behind the rotating cylinders, measured with hot wire probes.

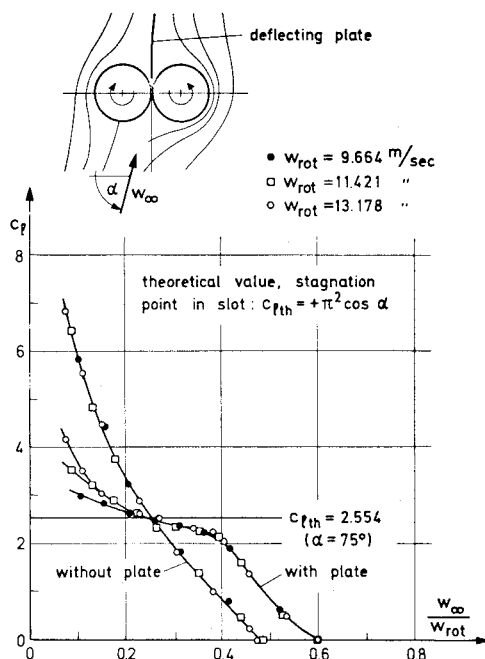


Fig. 8 Influence of a deflecting plate behind the cylinders. The theoretical values for  $\alpha_r = 180$  deg can be achieved.

stagnation point located in the slot between the two cylinders as shown in Fig. 3. This condition is valid for one ratio  $w_\infty/w_{rot}$  only and is therefore not generally applicable. In the region of  $52.5 \text{ deg} \leq \alpha \leq 90 \text{ deg}$  (lefthand side of Fig. 6), no pressure drag was measured for  $w_\infty/w_{rot} \leq 0.40$ . In the case of  $\alpha = 90 \text{ deg}$  where no lift force is generated, the optimum

velocity ratio based on the drag measurements was  $w_\infty/w_{rot} = 0.405$ .

The lift coefficients  $c_l$  in the region  $0 \text{ deg} \leq \alpha \leq 45 \text{ deg}$  (righthand side of Fig. 6) show a different behavior indicating that viscous forces degrade the lift-to-drag ratio of the cylinders. Large portions of the cylinder walls move against the general flow direction causing local flow separations to occur. At  $\alpha < 75 \text{ deg}$  the measured lift exceeded the maximum theoretical value of  $c_{lth} = 9.87$ . However, the measurements at the corresponding very low ratios  $w_\infty/w_{rot}$  are not so accurate due to the low flow velocity (on the order of 1 m/s or less). Of course the jet formed by the cylinder boundary layer should cause some additional lift.

In order to understand the flow conditions at the rear stagnation point the velocity distribution behind the cylinders was measured with hot wire probes (Fig. 7). The profile of the jet for different flow velocities shows a distinct displacement to the right towards the freestream flow direction when  $w_\infty$  is increased. At low free stream velocities the jet determines the location of the outgoing streamline and thereby the whole flowfield. This is confirmed by tests with a deflecting plate attached to the wind tunnel wall and located just behind the cylinders (Fig. 8).

The curve is approaching the theoretical value  $c_{lth} = 2.554$  for decreasing  $w_\infty/w_{rot}$  with the exception of very low ratios of  $w_\infty/w_{rot}$ , where again the jet produced by the rotating cylinders dominates the flow.

### Concluding Remarks

The flow around two rotating cylinders inclined to the flow direction is governed by the jet formed by the boundary layers on the two cylinders and associated interaction with the external flowfield. For velocity ratios  $w_\infty/w_{rot} \leq 0.4$  and for angles of attack  $90 \text{ deg} < \alpha < 52.2 \text{ deg}$ , the tests indicate a greatly reduced or eliminated pressure drag.

A new concept of stagnation point control is demonstrated that is not based upon avoiding flow separation (the Kutta-Joukowski condition) as on the single rotating cylinder, but rather depends on the effect of the momentum of the two boundary layers of the rotating cylinders forming a jet that defines the downstream flow conditions.

### References

- 1Bridel, G., and Thomann, H.H., "Wind Tunnel Balance Based on Piezoelectric Quartz Force Transducers," *Journal of Aircraft*, Vol. 17, May 1980, pp.
- 2Bridel, G., "Strömungsuntersuchungen an 2 rotierenden Zylindern mit einer neuen Mehrkomponentenwaage," Thesis No. 6108, Swiss Federal Institute of Technology, Zurich, Switzerland.

## Aircraft Configuration Optimization for Ground Attack Mission

P. Ramamoorthy\* and A. K. Sinha\*

National Aeronautical Laboratory, Bangalore, India

- $R$  = wing aspect ratio
- $C_{D0}$  = profile drag coefficient
- $C_{DB}$  = base drag coefficient
- $C_{DF}$  = skin friction drag coefficient
- $C_{DW}$  = wave drag coefficient
- $C_L$  = lift coefficient

Received Aug. 20, 1979. Copyright © American Institute of Aeronautics and Astronautics, Inc., 1979. All rights reserved.

Index categories: Configuration Design; Performance; Aerodynamics.

\*Scientist, Aerodynamics Division.